THE JOURNAL OF BIOLOGICAL CHEMISTRY
Vol. 275, No. 45, Issue of November 10, pp. 35013–35020, 2000
Printed in U.S.A.

Acetylation Increases the α-Helical Content of the Histone Tails of the Nucleosome*

Received for publication, June 8, 2000, and in revised form, August 1, 2000
Published, JBC Papers in Press, August 9, 2000, DOI 10.1074/jbc.M004998200

Xiaoying Wang, Susan C. Moore, Mario Laszckzak, and Juan Ausió‡

From the Department of Biochemistry and Microbiology, University of Victoria, Victoria V8W 3P6, British Columbia, Canada

The nature of the structural changes induced by histone acetylation at the different levels of chromatin organization has been very elusive. At the histone level, it has been proposed on several occasions that acetylation may induce an α-helical conformation of their acetylated N-terminal domains (tails). In an attempt to provide experimental support for this hypothesis, we have purified and characterized the tail of histone H4 in its native and mono-, di-, tri-, and tetra- acetylated form. The circular dichroism analysis of these peptides shows conclusively that acetylation does increase their α-helical content. Furthermore, the same spectroscopic analysis shows that this is also true for both the acetylated nucleosome core particle and the whole histone octamer in solution. In contrast to the native tails in which the α-helical organization appears to be dependent upon interaction of these histone regions with DNA, the acetylated tails show an increase in α-helical content that does not depend on such an interaction.

The identification of histone acetyltransferases as integral components of transcriptional eukaryotic complexes (1) has renewed interest in histone acetylation; however, the precise structural role of this important post-translational modification remains elusive. Initial hypotheses proposed that this modification was responsible for weakening histone-DNA interactions, thereby producing a more "open" chromatin conformation, but the situation does not appear to be that simple.

At the chromatin fiber level, in the absence of linker histones, histone acetylation induces an extended chromatin conformation (2), which is more amenable to transcription. However, when the full complement of histones is present, the extent of folding of the fiber does not appear to be greatly affected by this post-translational modification (3, 4).

At the nucleosome level, the acetylated particle adopts a more asymmetric structure (5). This is mainly the result of the DNA ends flanking this chromatin particle binding less tightly to the histones and adopting a stretched conformation (2, 6). As ionic strength is increased, acetylated histone tails are more readily released from DNA interaction(s) (7) than their nonacetylated counterparts. This is as expected and is a consequence of the charge neutralization resulting from acetylation. However, under physiological ionic conditions, the histone tails are persistently bound (7) to the nucleosome regardless of the extent of acetylation. Thus, not surprisingly, the evidence in support of histone acetylation facilitating the binding of transcription factors to nucleosomally organized DNA has been very controversial (8–10). In fact, it has recently been shown that binding of the developmental transcription factor HNF3, which preferentially binds to nucleosomal DNA, is not affected by histone acetylation (11). A more recent hypothesis proposes that histone acetylation provides a histone code (12). However, the structural changes associated with this code remain undefined.

The tails of the core histones have been shown to adopt a helical conformation in nucleosomal DNA (13). However, it was not made clear whether the helical conformation preexisted in the histone tails or was a result of their interaction with DNA. Early studies (14) have also indicated that histone acetylation increases the overall α-helical content of these proteins in a way that was not defined. Given the relevance of both acetylation and the histone tails in the processes of chromatin folding (2, 15–17) and the regulation of gene expression (18), we decided to determine the structural effect of acetylation on these histone domains.

Finally, it has been recently postulated that the spacing of the acetylatable lysine residues of the H3-H4 histone tails is "reminiscent of that of an α -helix" (12). This is an idea first proposed 30 years ago by Sung and Dixon (19). This paper represents the first experimental evidence that such a postulate is indeed correct.

MATERIALS AND METHODS

Cell Cultures and Tissues—MSB cells (chicken erythroleukemic cells transformed by Marek's virus) were kindly provided to us by Dr. Vaughn Jackson. The cells were grown in 5% fetal calf, 5% newborn serum in 1:1 Dulbecco's modified Eagle's medium/RPMI 1640 medium supplemented with 50 mM HEPES, 30 mM bicarbonate, and 2 mM glutamine as described previously (20). The cells where grown to a density of 1–2 × 10^6 cells/ml and then were harvested or incubated in the presence of 5 mM sodium butyrate for 20–22 h before harvesting. After harvesting (3800 × *g* for 10 min at 4 °C), the cell pellets were suspended in 0.5 Dulbecco's modified Eagle's medium, 40% glycerol at a density of approximately 2 × 10^7 cells/ml, and the suspension was stored at −80 °C until further use. Chicken erythrocytes were used as a source of native and trypsinized nucleosomes.

Chromatin Preparation—The cell suspension was thawed and centrifuged at 3800 × *g* for 15 min at 4 °C. The pellets were resuspended in buffer A (0.25 M sucrose, 60 mM KCl, 15 mM NaCl, 10 mM MES[1] (pH 6.5), 5 mM $MgCl_2$, 1 mM $CaCl_2$, 0.5% Triton X-100, with or without 10 mM sodium butyrate) at a ratio of 5 ml/g of pellet using a disposable plastic transfer pipette. The suspension was then centrifuged at 3000 ×

* This work was supported by Medical Research Council of Canada Grant MT-13104 (to J. A.). The costs of publication of this article were defrayed in part by the payment of page charges. This article must therefore be hereby marked "*advertisement*" in accordance with 18 U.S.C. Section 1734 solely to indicate this fact.

‡ To whom all correspondence should be addressed: Dept. of Biochemistry and Microbiology, University of Victoria, P.O. Box 3055, Petch Bldg. 220, Victoria, British Columbia V8W 3P6, Canada. Tel.: 250-721-8863; Fax: 250-721-8855; E-mail: jausio@uvic.ca.

[1] The abbreviations used are: MES, 4-morpholineethanesulfonic acid; Pipes, 1,4-piperazinediethanesulfonic acid; AU, acetic acid-urea; HPLC, high performance liquid chromatography; PAGE, polyacrylamide gel electrophoresis; RP-HPLC, reversed-phase high performance liquid chromatography; TFE, trifluoroethanol.

g for 10 min at 4 °C. This step was repeated once more, and the pellets were next resuspended in 20 ml of buffer B (50 mM NaCl, 10 mM Pipes (pH 6.8), 5 mM $MgCl_2$, 1 mM $CaCl_2$, with or without 10 mM sodium butyrate) and centrifuged under the same conditions described above. The nuclear pellets were resuspended again in buffer B (10 ml) using a transfer pipette, and the DNA concentration of the suspension was adjusted to A_{260} = 40, using the same buffer. The DNA concentration was determined by lysing a small aliquot of the nuclear suspension in a 200-fold excess of distilled water followed by the addition of 10% SDS to a final concentration of 0.5%. The nuclear suspension was then incubated at 37 °C for 10 min and digested at this temperature for an extra 5–6 min with micrococcal nuclease (Worthington) at 50 units/ml. The digestion reaction was stopped by the addition of 500 mM EDTA to a final EDTA concentration of 10 mM (on ice) and centrifuged at 10,000 × *g* for 10 min at 4 °C. The supernatant of this "fraction a" consists mainly of highly hyperacetylated mononucleosomes (usually containing 15–20 mg of DNA). This fraction was stored on ice in the presence of 1:100 (v/v) (protease inhibitor mixture; see below). The pellets were suspended in 15 ml each of buffer C (100 mM NaCl, 10 mM Pipes (pH 6.8), 5 mM $MgCl_2$, 1 mM $CaCl_2$), with or without 10 mM sodium butyrate plus protease inhibitor mixture "Complete" from Roche Molecular Biochemicals; one pill was dissolved in 1 ml of water and used at 1:100 (v/v). The chromatin extraction was carried out by pipetting up and down with a 10-ml glass pipette until completely homogeneous. This was incubated for 30 min on ice with occasional vortexing and centrifuged at 10,000 rpm for 10 min to produce a supernatant (fraction b). This fraction usually yields 8–10 mg of DNA and consists of oligonucleosomes in which the histones are still highly hyperacetylated. The chromatin extraction was repeated once more but using buffer D (350 mM NaCl, 10 mM Tris-HCl (pH 7.5), 5 mM $MgCl_2$, 2 mM EGTA, with or without 10 mM sodium butyrate plus protease inhibitor) in the same way as for buffer C. This gives a poorly acetylated fraction that typically contains 20 mg of DNA. The compositions of the buffers are the same as those described by Perry and Chalkley (5, 21).

Chicken erythrocyte nucleosome core particles were prepared as described previously (22). Trypsinized nucleosome core particles were also prepared as described previously (22) except that L-1-tosylamido-2-phenylethyl chloromethyl ketone-treated trypsin immobilized on beaded agarose was used (Pierce). Nucleosomes at an A_{260} = 10 that had been dialyzed against buffer E (25 mM NaCl, 10 mM Tris-HCl (pH 7.5)) were mixed with a pre-equilibrated trypsin suspension (200 *p*-tosyl-L-arginine methyl ester units per ml of suspension at a ratio of 1 ml of trypsin suspension/300 A_{260}). For the equilibration of the trypsin suspension, the volume of suspension needed was washed by centrifugation five times with 3 volumes of buffer E. After the last wash, the nucleosome sample was added to the trypsin pellet and allowed to tumble for 50–60 min at room temperature. The immobilized trypsin was then removed by centrifugation, and the "Complete" protease inhibitor mixture was added to the supernatant in a 1:100 (v/v) ratio. The sample was then concentrated to an A_{260} = 50–60 using a Centriprep-50 (Amicon-Millipore, Millipore Corp., Bedford, MA) and loaded on a 5–20% sucrose gradient in buffer E and run at 100,000 × *g* for 20 h at 4 °C. After collection of the fractions, the nucleosome peak was dialyzed against buffer E containing 0.1 mM EDTA and was stored on ice until further use.

Gel Electrophoresis—Native PAGE for the analysis of nucleosomes and DNA was carried out as described in Ref. 23. SDS-PAGE was carried out according to Laemmli (24). Acid-urea (AU) PAGE was carried out as described elsewhere (5).

Histone Isolation and Fractionation—Fractions a, b, and c were brought to a final NaCl concentration of 350 mM by the addition of 5 M NaCl and were loaded onto a hydroxylapatite column (Bio-Gel HTP, DNA grade; Bio-Rad) that had been equilibrated in 0.1 M potassium phosphate (pH 6.8) buffer (25, 26). After loading the sample, the column was run overnight at room temperature in 0.35 M NaCl, 0.1 M potassium phosphate (pH 6.8), and the H2A-H2B and H3-H4 histones were eluted with a 0.35–2 M NaCl gradient in the same buffer. Columns of different sizes were used and eluted with a 6-column volume gradient at room temperature. The peak containing H3-H4 was exhaustively dialyzed at 4 °C against distilled water using Spectra/Por 3 membrane (Spectrum laboratories Inc., Houston, TX) and lyophilized. Histones H3 and H4 were fractionated by reversed-phase HPLC (27) on a Vydac C_4 (5 μm) 1.0 × 25-cm column (Vydac, Hesperia, CA) with a 0–60% acetonitrile gradient in 0.1% trifluoroacetic acid at a flow rate of 2 ml/min. The peak containing the highly acetylated H4 fractions was lyophilized.

Histone octamers (native, trypsinized, and acetylated) were prepared from their respective nucleosome counterparts. To this purpose, the nucleosome core particles (~2–3 mg) in buffer E, prepared as described above were loaded onto small hydroxylapatite columns (1.0 × 6 cm) equilibrated in 0.1 M potassium phosphate buffer. The column was washed with 2 volumes of 0.35 M NaCl in 0.1 M phosphate buffer (pH 6.8), and the histone octamers were eluted with 2 M NaCl in the same buffer. Elution and loading were carried out at a flow rate of 12 ml/h.

Preparation of Histone H4 Tails with Different Extents of Acetylation—Acetylated and control (nonacetylated) H4 were digested with endoproteinase Asp-N (EC 3.4.24.33) (Roche Molecular Biochemicals) in either 100 mM ammonium bicarbonate (pH 8.0) or 50 mM Tris-HCl (pH 6.0) at room temperature with an enzyme/substrate ratio of 1:1500 (w/w). Endoproteinase Asp-N cleaves the protein at the N-terminal site of aspartic acid with differing specificity depending on pH. Immediately after digestion, the sample was directly loaded onto a reversed-phase HPLC Vydac C_{18} (5-μm) 0.46 × 25-cm column (Vydac, Hesperia, CA) and was eluted with a linear acetonitrile gradient in 0.1% trifluoroacetic acid at a flow rate of 1 ml/min. The fractions corresponding to the non-, mono-, di-, tri-, and tetraacetylated H4 tail were collected and lyophilized.

Amino Acid Analysis—Amino acid analyses were carried out on an ABI model 420A derivatizer analyzer system as described elsewhere (28).

Determination of Protein and DNA Concentrations—The absorption coefficient of the native core histones was A_{280} = 0.45 cm^2 mg^{-1} (14). The molecular weight of the native histone octamer (10.8 × 10^4 g/mol) and that of the trypsinized octamer (8.8 × 10^4 g/mol) were calculated from the amino acid sequences of the individual histones and from the data reported by Böhm and Crane-Robinson (29) on trypsinized histones as described in Ref. 22. All of the analyses were carried out in triplicate. A value of 3200 cm^{-1} mol^{-1} was used for the molar extinction coefficient of the histone tails (30) at 205 nm. Using a comparative amino acid analysis with an internal norleucine standard, no significant variation of the extinction coefficient resulting from the addition of the acetyl groups could be detected at this wavelength. DNA concentrations were determined using A_{260} = 20.0 cm^2 mg^{-1}. The molecular weight of the 145-base pair nucleosome core particle DNA was taken to be 9.6 × 10^4 g/mol. The absorption coefficient of the native nucleosome core particles was A_{260} = 9.5 cm^2 mg^{-1} (31), and that of the trypsinized nucleosome core particles was A_{260} = 10.5 cm^2 mg^{-1}. For this latter calculation, the absorption coefficient of the trypsinized histone octamer at 260 nm was considered to be the same as that of the native histone octamer (A_{260} = 0.23 cm^2 mg^{-1}) (32).

Circular Dichroism—Circular dichroism spectra were recorded at 20 °C on a Jasco J-720 spectropolarimeter as described previously (5). The nucleosomes and the histone octamers were dialyzed against the different buffers described here. The histone tails were dissolved directly in the corresponding buffers or in 90% TFE. Nucleosome and DNA samples were analyzed in 1-cm path length cells, and histone and H4 tail spectra were taken in 0.1-cm cells.

For the calculation of the mean residue molecular ellipticity [θ], an average M_r value of 110.6 was used for the calculation of the main molecular residue ellipticity of the native histone octamer and 110.4 for the trypsinized histone octamer as determined from amino acid analysis of these two proteins. In the case of the histone H4 tail, M_r values of 103.2, 105, 106.6, 108.4 and 110.2 were used for the non-, mono-, di-, tri-, and tetraacetylated forms, respectively, as calculated from the amino acid sequence. The average M_r (for a nucleotide) used for the DNA was 331.

Secondary Structure Prediction—Secondary structure prediction was carried out with the help of the DNASTAR Program (DNASTAR Inc., Madison, WI) using the Protean analysis system tool.

Because core histones exhibit a very low β sheet structure (33, 34), the percentile of α-helix was calculated from either the values of the ellipticity [θ] at either 220 nm according to Ref. 30 using the relation,

$$\alpha = 8.9 - 2.4 \cdot [\theta]_{220} \cdot 10^{-3} \quad \text{(Eq. 1)}$$

or at 222 nm according to the following relation.

$$\alpha = -3.1(1 + [\theta]_{222} \cdot 10^{-3}) \quad \text{(Eq. 2)}$$

In the latter case, the relation was also established on the assumption that only random coil and helical regions were present. An average random coil ellipticity value of $[\theta]_{222}$ = 1000° (35) was used for the random coil contribution. For the α-helix, we used the average of the ellipticity values of helices of an average length of about 12 residues ($[\theta]_{222}$ = −30,000°) (36) and of α-helices of an average length of about 20 residues ($[\theta]_{222}$ = −35,500°) (37) as it pertains to the histone fold structure (33, 34).

RESULTS

The Far UV Region of the Nucleosome Spectrum Can Be Reliably Used to Determine the Spectrum of the Histone Octamer—Fig. 1 summarizes the experimental approach followed in this paper. It was designed in a way that would allow analysis of the secondary structure of the histone octamer and selectively look at the conformation of its N-terminal domains (tails) in the presence or absence of interaction with the nucleosomal DNA. The electrophoretic characterization of the DNA, nucleosome, and histone components is shown in Fig. 2.

Fig. 3*A* shows the circular dichroism spectra of native and trypsinized chicken erythrocyte nucleosome core particles as well as that of their constitutive 145-base pair DNA. The histone octamer has a strong contribution to the far UV region of the spectrum, whereas the DNA component exerts its main contribution in the near UV region (see Fig. 3*A*, *inset*). The spectra of the trypsinized nucleosome and that of the native counterpart in the near UV region are identical to those reported earlier (22) with an ellipticity increase (~17%) at the maximum (282.5 nm) within this region of the spectrum for the trypsinized nucleosomes.

As is shown in Fig. 3*B*, it is possible to subtract the DNA contribution to the far UV region of the spectrum from that of the nucleosome and obtain a protein spectrum that is very similar to the spectrum of the histone octamer in a high salt concentration solution (2 M NaCl) in which the histone octamer exists as a stable entity (33, 38). The similarity of the two spectra shown in this figure is remarkable. The ellipticity of the octamer in the nucleosome form was calculated from the concentration of nucleosomes using the absorption coefficient of DNA (A_{260} = 20.0 cm^2 mg^{-1}) assuming 1 mol of histone/mol of DNA and using M_r = 110.6. The ellipticity of the octamer in solution was calculated directly from the concentration of the protein using its absorption coefficient (14). Furthermore, the histone octamer spectra are almost identical to those previously reported for the histone octamer in 2 M NaCl (14). From the ellipticity values at 222 nm and using Equations 1 and 2, it is possible to estimate the amount of α-helix as 46.6 and 52.5%, respectively, for the histone octamer in the nucleosome and 43.7 and 48.7% for the histone octamer in 2 M NaCl. The values determined with Equation 2 compare very well with the value of 49.4% as determined from the crystallographic structure (34), assuming that the regions not visualized in that analysis (see Fig. 3*C*) did not have any α-helical structure.

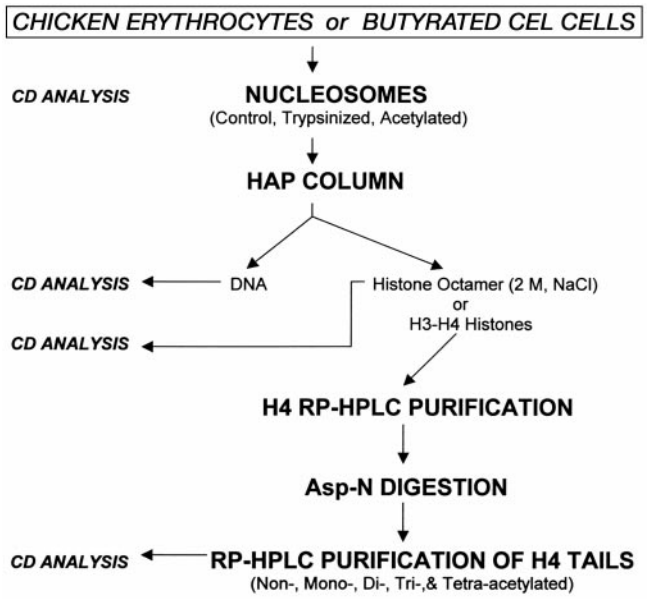

FIG. 1. **Experimental flow chart summarizing the fractionation and analysis of the DNA, nucleosome and histone components.**

The Far UV Spectra of Native and Fully Trypsinized Nucleosome Core Particles Are Very Similar—Once it was established that the far UV region of the CD spectrum of the nucleosome core particle could be reliably used to determine the secondary structure of its constitutive histone octamer, we decided to analyze the changes in the histone octamer resulting from the removal of the histone tails by immobilized trypsin.

It is interesting to note (see Fig. 3*A*) that the far UV region of the spectrum of the nucleosome for both the native and the trypsinized core particles look very similar, despite the differences observed in the near UV region (see Fig. 3*A*, *inset*). However, when this region of the spectrum for the trypsinized particles is normalized for the mass lost from the histone octamer as a result of trypsinization (see *thin dashed line* in Fig. 3*A*), then there is an increase in the ellipticity at 222 nm that corresponds to an 11.6% increase in the α-helical content of the trypsinized histone octamer (see also Fig. 3*B*). The α-helical content determined in this way is in good agreement with the corresponding value (62%) estimated from the crystallographic data (34). When the value of the α-helical content (64.4%) for the trypsinized core is combined with that estimated for the whole molecule (52.8%) and taking into consideration their relative molecular masses, it is possible to estimate the α-helical content of the tail domains to be approximately 17%. This

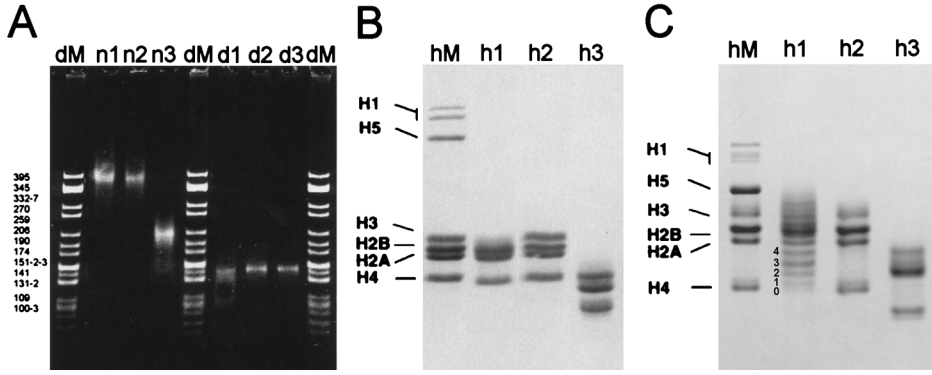

FIG. 2. **Electrophoretic analysis of the nucleosome core particles and their DNA and histone components.** *A*, native (4%) polyacrylamide gel of acetylated (*n1*), native (*n2*), and trypsinized (*n3*) nucleosome core particles and their corresponding constitutive DNA (*d1*, *d2*, and *d3*). *dM* is a DNA marker obtained by cutting pBR 322 with *Hha*I. *B*, SDS-PAGE of the acetylated (*h1*), native (*h2*), and trypsinized (*h3*) histones. *hM* are chicken erythrocyte histones used as a marker. Notice that the H3/H4 exhibit a slightly faster and more fuzzy appearance in this type of gel electrophoresis as a result of their acetylation levels (60). It is because of this that histone H3 appears underrepresented in these kinds of gels. *C*, AU-PAGE of the same histones shown in *B*. The *numbers* in *lane h1* indicate the number of acetylated lysines.

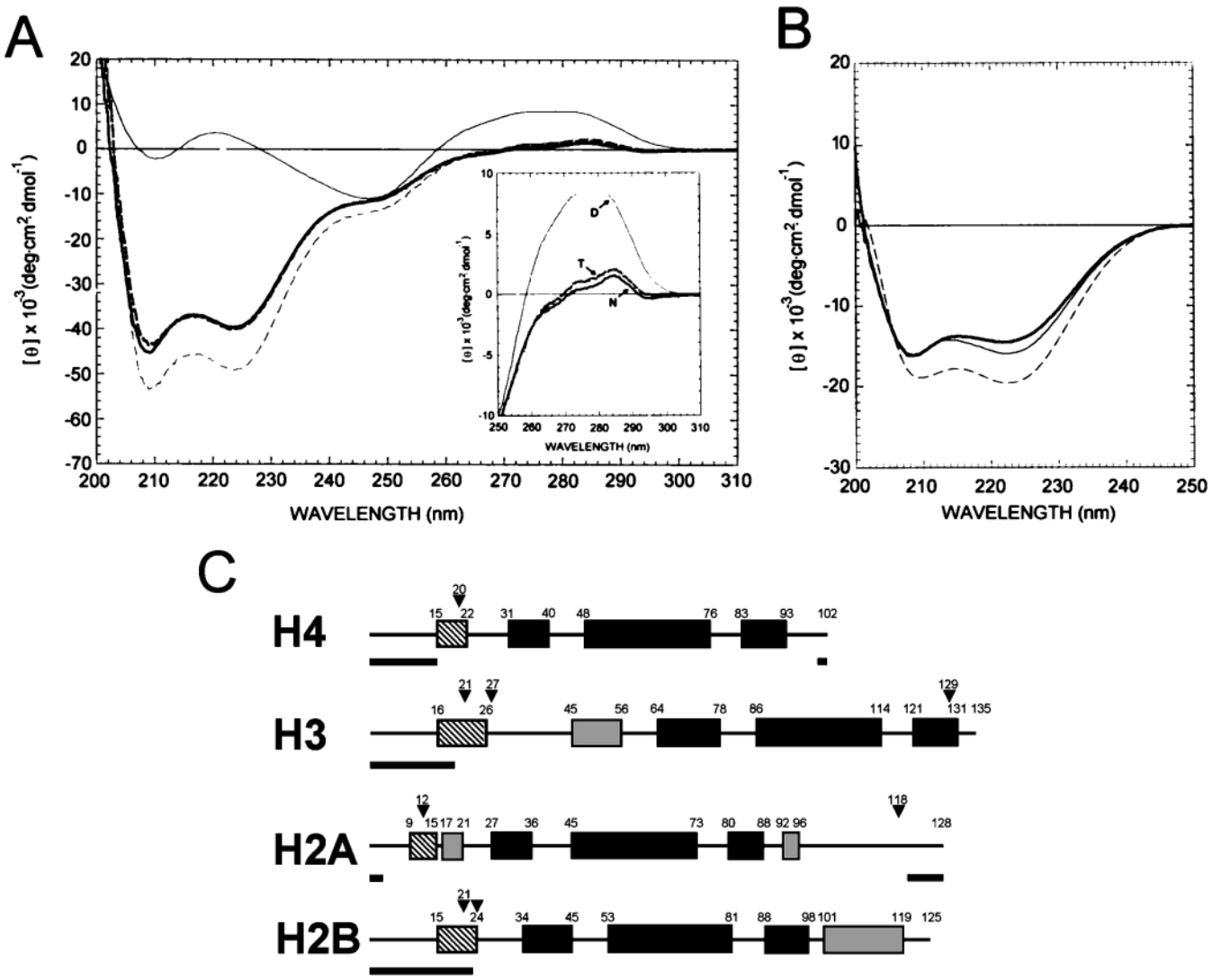

FIG. 3. *A*, CD spectra of native nucleosome core particles (*thick line*), trypsinized nucleosome core particles (*thick dashed line*), and nucleosomal DNA (*thin line*) in 25 mM NaCl, 5 mM Tris-HCl (pH 7.5). The *thin dashed line* corresponds to the CD for the trypsinized nucleosomes after normalization for the loss of mass due to the protein mass loss resulting from trypsin treatment. The *inset* represents an enlarged view of the near UV region portion of the same spectra. For clarity, the normalized spectrum of the trypsinized nuclesomes is not shown. *D*, DNA; *N*, native nucleosome core particles; *T*, trypsinized nucleosome core particles. *B*, CD spectra of the histone octamer in 2 M NaCl, 0.1 mM dithiothreitol, 10 mM Tris-HCl (pH 8.0) (*thick line*) and in the native (*thin line*) or trypsinized (*thin discontinuous line*) nucleosome core particle. The spectra of the octamer in the nucleosome core particle were obtained by subtraction of the nucleosomal DNA spectrum from that of the corresponding native or trypsinized nucleosome core particle shown in *A*, and they were corrected for the relative mean residue molecular weight of the amino acid (M_r = 110.4–110.6) *versus* that of the nucleotide (M_r = 331; see "Materials and Methods"). In the case of the trypsinized nucleosome core particle, the spectrum obtained in this way for the trypsinized octamer was also corrected for the loss of protein mass due to trypsinization. *C*, schematic representation of the α-helical structure of the core histones as determined from the crystal structure of the histone octamer (33) and the nucleosome (34). The *boxes* in *black* correspond to the "histone fold" (33). The *stippled boxes* correspond to the α-helical prediction by Fasman *et al.* (61). The *thick underlining* corresponds to the portions of the histones that could not be visualized in the crystal structure of the nucleosome (34).

value is considerably lower than the value of 30–35% previously estimated (13).

In an attempt to determine if the α-helical conformation of the tails is a result of their interaction with the nucleosomal DNA as it has been routinely hypothesized (13), we looked at the ionic strength variation of the spectrum of native nucleosome core particles in the range of 25–600 mM NaCl. Nucleosome core particles retain their integrity within this range of salt concentration (31), while the histone tails are presumably released from their interaction with nucleosomal DNA as the ionic strength increases (39). Although the near UV region of the spectra showed an increase at 282.5 nm, which is characteristic of the effect of the ionic strength increase within this range (22), the far UV spectrum remained virtually unchanged, and we could not determine any significant changes in the $[\theta]_{222}$ at any of the salt concentrations analyzed (results not shown).

Acetylation Increases the α-Helical Content of the Histone Octamer both in the Nucleosome and in Solution—It has been shown that the protein environment significantly affects the amino acid preference for secondary structure (40). Thus, the ionic environment and the electrostatic interactions of the histone tails with the nucleosomal DNA may have an important impact on the structure adopted by these histone domains in the nucleosome.

If the charge neutralization of the histone tails upon interaction with DNA is responsible for their α-helical conformation (13), then it would be expected that acetylation of the lysines in the tails should favor this conformation. To test this possibility, we prepared highly hyperacetylated nucleosome core particles

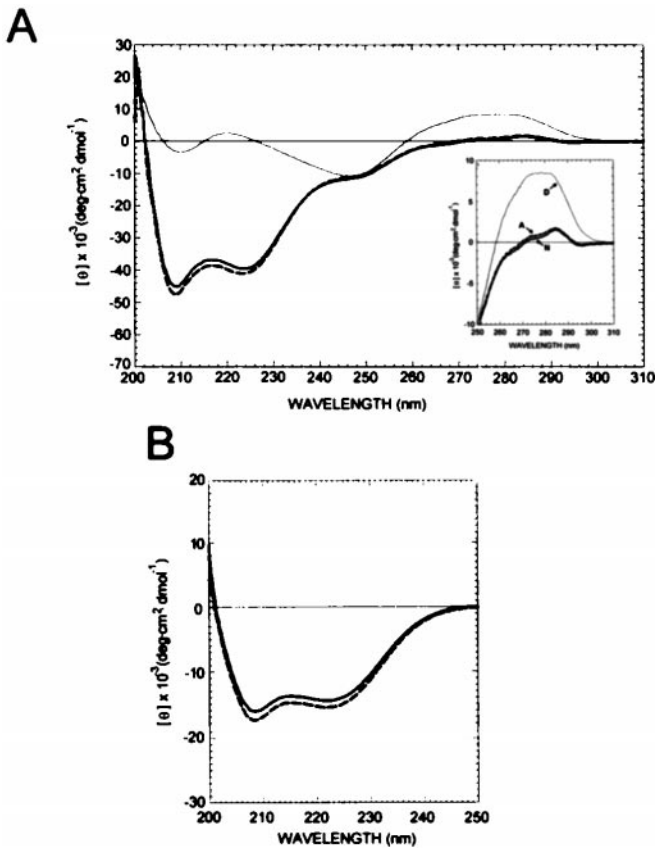

FIG. 4. *A*, CD spectra of native nucleosome core particles (*thick line*), acetylated nucleosome core particles (*thick dashed line*), and nucleosomal DNA (*thin line*). The *inset* represents an enlarged view of the near UV region portion of the same spectra. *A*, acetylated nucleosome core particles; *D*, DNA; *N*, native nucleosome core particles. *B*, CD spectra of the histone octamer in the native (*thick line*) and in the acetylated (*thick discontinuous line*) nucleosome core particle. These spectra were obtained in the same way as in Fig. 3*B*.

(5) and their corresponding histone octamers (see Fig. 2). To facilitate the structural comparison with the native counterparts, these particles were obtained from chicken erythroleukemic cells grown in the presence of butyrate (see "Materials and Methods" for more details).

Fig. 4, *A* and *B*, respectively, shows the CD spectra of hyperacetylated nucleosome core particles and histone octamers in comparison with their native counterparts. As we had reported earlier, histone acetylation increases slightly the ellipticity at the maximum at 282.5 nm in the near UV region of the nucleosome core particle spectrum (see Fig. 4*A*, *inset*) (5). The far UV region of the spectrum also exhibits a small (2–3%) but significant and very reproducible increase the negative ellipticity at 220–222 nm. Similarly the octamer also exhibits an enhanced ellipticity within this region (4–5%) when in 2 M NaCl solution. This latter value is in good agreement with the average 4.8% value previously reported by Prevelige and Fasman (14) for acetylated HeLa cell octamers in 2 M NaCl under a variety of different temperatures and concentrations. This clearly indicates that the α-helical content of the tails increases upon acetylation of their lysine amino acids. A 2–3% overall increase corresponds to a 11–17% increase in the α-helical content of the histone tails. When this value is combined with that described above (17%), the overall increase in the α-helical content of the tails as a result of acetylation increases by 64–100%.

The α-Helical Content of the Histone Tails Increases with the Number of Acetylated Lysines—In order to further analyze the effects of acetylation on the histone tails, we isolated the histone tail of histone H4 with different extents of histone acetylation. Histone H4 purified from either chromatin fraction b or c from butyrate treated cells (see "Materials and Methods") was digested with Asp-N endopeptidase, and the resulting peptides were fractionated by reversed-phase HPLC (see Fig. 5). As seen in Fig. 5*A*, *lanes 1* and *2*, the products of the digestion vary depending on the pH of the buffer used. We found that at low pH (pH 6.0), the digestion proceeds more efficiently than at pH 8.0, and the lower pH conditions result in the production of a peptide (see *arrowhead*) that runs very close to the tetraacetylated form of peptide 1–23 in AU-PAGE and co-elutes with it in the HPLC. Therefore, we routinely digested H4 at pH 8.0. The elution pattern shown in Fig. 5*B* corresponds to acetylated histone H4 from chromatin fraction b digested under basic conditions. As can be see in Fig. 5*C*, this allows the complete purification and isolation of the different acetylated forms of the peptide 1–23, corresponding to the histone tail of H4. It is important to notice that each of the acetylated forms of the histone H4 tail elutes as multiple peaks (see Fig. 5*B*) except for the nonacetylated form. We attribute this complex elution profile to the different disposition of the multiple acetyl groups within each form and to the high resolution power of RP-HPLC. However, it is also possible that some of these bands could correspond to acetylated fractions that are additionally methylated at lysine 20.

Next, we analyzed the CD spectra of each of these acetylated forms both in the presence of TFE (a well known α-helix stabilizer) (Fig. 6*A*) and in aqueous solution (Fig. 6*B*). As seen in Fig. 6*A*, the histone H4 tail adopts an α-helical conformation in TFE. In contrast, in aqueous solution, these peptides display a spectrum that is clearly characteristic of a random coil (37) as it had already been reported (41). The amount of α-helix in the native nonacetylated form, as calculated from Equations 1 and 2, is approximately 17% and exponentially increases to about 24% in the tetraacetylated form (see Fig. 6*C*). In the aqueous solution, there is a decrease in the intensity of the negative band at 195 nm, which is most likely the result of some protein compaction resulting from the charge neutralization effects of acetylation (see Fig. 6*D*).

DISCUSSION

The Tails of the Histones Adopt an α-Helical Conformation upon Binding to DNA in the Nucleosome—The value of 48.7% (using Equation 2; see "Materials and Methods") for the α-helical content of the histone octamer in solution as determined from the CD spectrum (see Fig. 2*B*) is in surprisingly good agreement with the value of 49.4% determined from the crystal structure (34). Such excellent agreement is most likely due to the fact that the secondary structure of the core histones consists almost exclusively of α-helix and random coil, and both Equations 1 and 2 are based on peptide models consisting of these two structures. Equation 1 (30) is based on information from polylysine data (42). Equation 2, in principle, should provide better estimates for histones because it was empirically derived from the analysis of globular proteins and is based on α-helices of 10–20 residues, a size that corresponds to those found in histones (see "Materials and Methods").

We have consistently found that the α-helical content of the histone octamer in the nucleosome appears to be slightly higher (~4%). If we assume that the extinction coefficients for DNA and histones were both determined with similar accuracy, then this difference is as expected from and could be attributed to the histone tails adopting a 15–20% increase in helical content upon binding to DNA. This is consistent with the α-helical content of the tails as determined from the analysis of trypsinized nucleosomes described above (see also Fig. 2*B*) and suggests that the helical conformation of the tails is the result

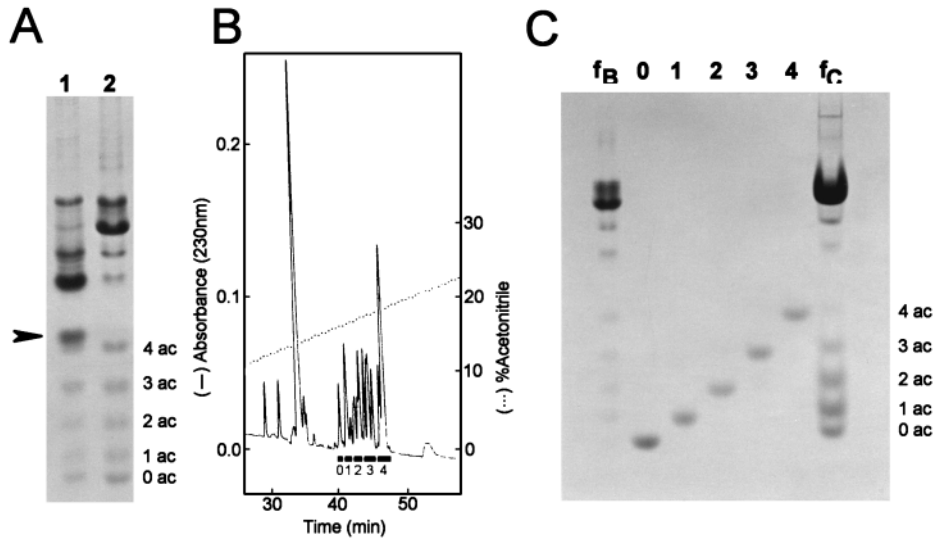

FIG. 5. *A*, AU-PAGE analysis of the peptides obtained upon digestion of acetylated histone H4 (obtained from chromatin fraction c; see "Materials and Methods") with Asp-N endoproteinase in 50 mM Tris-HCl (pH 6.0) (*lane 1*) or 100 mM ammonium bicarbonate (pH 8.0) (*lane 2*). The *arrow* points to an internal peptide that elutes in RP-HPLC in the same position as the tetraacetylated N-terminal peptide (amino acids 1–23). *B*, RP-HPLC elution profile of the products of digestion of acetylated histone H4 (obtained from fraction b) with Asp-N endoproteinase at pH 8.0. *C*, AU-PAGE analysis of *peaks 1–4* from *B*. f_B, acetylated histone H4 (obtained from fraction b); f_C, acetylated histone H4 (obtained from fraction b) upon digestion with Asp-N endoproteinase at pH 8.0.

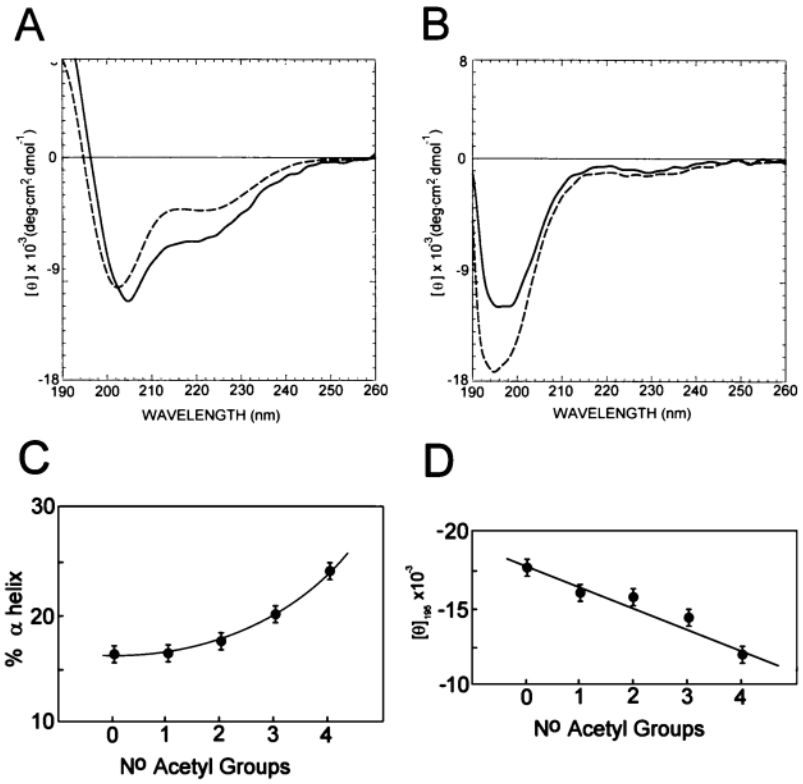

FIG. 6. *A*, CD spectra of the native (*solid line*) or tetraacetylated (*discontinuous line*) form of the N-terminal peptide (amino acids 1–23) of histone H4 in 90% TFE. *B*, same as in *A* but in 25 mM NaCl, 5 mM Tris-HCl (pH 7.5). *C*, dependence of the α-helical content of the histone H4 tail on the number of acetylated residues present in this region. The amount of α-helix was determined from the spectra such as those shown in A (in 90% TFE), using Equation 2. *D*, variation of the ellipticity at 195 nm as a function of the extent of acetylation of the histone H4 tail in aqueous solution (*B*).

of their interaction with DNA as previously hypothesized (13). However, the estimate of the helical content resulting from this interaction is about half the value determined using nucleosome core particles that had been proteolyzed to different extents with clostripain (13). While the reason for such a difference is not completely clear, it may reflect experimental differences in the proteolysis experiments, both in terms of the different enzymes and the nature of the enzymes used. We have already described and discussed the importance of using immobilized proteases for such analyses (22) and have shown that the use of free trypsin can lead to overdigestion during storage of nucleosome core particles prior to their analysis. Based on this possibility, Fig. 3*C* can be used to illustrate this. While the regions predicted to be in an α-helical conformation (*stippled boxes*) within the N-terminal domains of the histones amount to approximately 40–45%, the amount corresponding to the tails removed by trypsin is about 20–25%, which is in agreement with our experimental determinations.

It has been shown that increasing the salt from 0.2 to 0.6 M NaCl causes the tails of the histones to dissociate completely from the nucleosomal DNA (39). Therefore, if the histone-DNA interactions play a role in the α-helical conformation, it would be expected that their salt-dependent dissociation would lead to a decrease in the band at 220–222 nm of the spectrum.

FIG. 7. *A*, amino acid sequence of the peptide generated by Asp-N endoproteinase digestion of histone H4 (residues 1–23). The *asterisks* indicate the sites of acetylation. *B*, predicted α-helical domains using different secondary structure prediction methods. *I*, Chou and Fasman (62); *II*, double prediction method (63); *III*, Gilbrat method (64); *IV*, α-amphipathic regions (Eisenberg *et al.* (65)); *V*, α-helical consensus from the four prediction methods. The increase in darkness reflects the increasing amount of consensus. *C*, schematic representation of the N-terminal 23 amino acids of histone H4 in an extended conformation (*I*) and after the region highlighted in *B* (*V*) has adopted an α-helical conformation (*II*). The distance between the *vertical marks* corresponds to the distance between adjacent amino acids in a fully extended chain (~3.63 Å) (66). For the α-helical conformation shown in *V*, the translation per residue within the helix it was considered to be 1.50 Å (66). *D*, helical wheel representation of the 23 N-terminal amino acid residues of histone H4. The *highlighted* amino acids correspond to the *shaded region* shown in *B* (*V*), and the background for the amino acids corresponds to the backgrounds shown in the same region.

Unfortunately, the salt-dependent variation of the far UV region of the CD spectra of nucleosomes did not provide the experimental support expected, since no change could be observed in this region of the spectrum as the salt was increased from 200 to 600 mM NaCl. However, as seen in Fig. 3*C*, the regions of the tails predicted to have helical potential are close to the histone boundaries defined by the trypsin digestion. The use of free trypsin in preparing trypsin-digested chromatin controls in earlier experiments (39) could have easily led to an overestimate of the effects due to these domains.

Despite all of this, the question still remains regarding the lack of structure found within the portions of the tails that could be visualized by crystallographic analysis. As extensively discussed in Ref. 13, this probably has to do with both the stringent conditions used in the preparation of the nucleosome crystals and the use of polyamines, which may have affected these histone domains.

Lysine Acetylation Increases the α-Helical Content of the Tails Regardless of Its Interaction with DNA—The results with acetylated nucleosome core particles and acetylated octamers (see Fig. 4, *A–B*) conclusively show that histone acetylation increases the α-helical content of the histone tails. The fact that this occurs both in solution and when bound to DNA suggests that such an increase is not dependent on the interaction of the affected regions with DNA. This supports observations from the analyses of model peptides, which have shown that the removal of the lysine side chain charges by acetylation stabilizes the helical structure (43).

Furthermore, the CD spectrum of the histone H4 tail containing different extents of acetylation in the presence of TFE (see Fig. 6) shows that the α-helical content increases exponentially with the extent of acetylation. TFE has been shown to selectively stabilize regions of peptides that have a propensity to adopt α-helical conformation in solution (44–47). From the maximum extent of this increase, the amount of α-helices in the absence of acetylation, and the predicted consensus helical region of histone H4 (see Fig. 7*B*), we can conclude that lysine 16 upon acetylation is the most likely residue to be responsible for such an increase (17–24%), and the region spanning amino acids 15–21 is the most likely candidate for producing the overall helical content of the histone H4 tail observed. If this is the case, the probability of this particular residue having an acetyl group would be expected to increase exponentially with the overall number of acetylated lysines present in this region, as it is indeed observed. Acetylation of lysine 16 in calf thymus histone H4 was shown to provide an altered CD spectrum for *in vitro* reconstituted histone H4-DNA complexes (48).

The fact that lysine 16 is involved in this process is very interesting, since this particular lysine is involved in the overactivation of one of the X chromosomes, which leads to dosage compensation in insects (49). Very recently, an MSL complex has been described in *Drosophila* that acetylates histone H4 at lysine 16 (50). Furthermore, the helical region highlighted in Fig. 7*B* corresponds to the region were amino acid insertions and deletions in yeast H4 are most detrimental to silencing (51).

Are the Changes in the α-Helical Content Induced by Acetylation Structurally and Functionally Relevant?—The results presented in this paper provide the first experimental evidence for acetylation increasing the α-helical content of the histone tails in chromatin. It is interesting to note that this was proposed by Sung and Dixon as early as 1970 (19), before the nucleosome structure had even been described. A similar postulate has also been recently proposed by Strahl and Allis (12). Although our results do not support an effect as extensive as those postulated by these papers, it is important to point out that acetylation may also operate in conjunction with other post-translational modifications such as phosphorylation. A quick inspection of Fig. 7*D* reveals that phosphorylation of serine 1 in histone H4 could neutralize arginines 3 and 19 if these two residues were part of a helix. Thus, it is possible that acetylation of all of the lysines (or most of them) in conjunction with phosphorylation of this serine could induce a much more dramatic increase in the helical content of this region than what we observed in the presence of acetylation alone. Indeed, it has been shown that during the replacement of histones by protamines during spermiogenesis in rainbow trout, histone H4 becomes extensively acetylated (52) and serine 1 is phosphorylated (19).

In the case of histone H4, the increase in α-helix due to acetylation of lysine 16 would represent a shortening of the span of interaction with DNA of approximately 4 Å (see Fig. 7*C*). Although this is a relatively small change, we anticipate that such an effect may be more pronounced in other histones such as histone H3, where the predicted α-helical region spans a longer amino acid range (positions 16–26; see Fig. 3*C*) and

encompasses two of the acetylatable lysines. Similarly, the α-helical region predicted for histone H2B (amino acids 15–24) includes three of the acetylatable lysines in this protein. These relatively small decreases in the span of histone-DNA interactions may cumulatively participate in the release of the flanking DNA regions (18 base pairs) of the nucleosome that has been shown to occur upon acetylation (5, 6). It is important to point out that while acetylation has been shown to play an important role in weakening the interaction of the histone tails with the nucleosomal DNA (53, 54), which is consistent with the decrease in the positive charge of the tails, the actual decrease observed for the binding constant (53) cannot account for the release of the flanking DNA ends. In fact, such a release can be observed under physiological buffer conditions in which the acetylated tails are still bound to DNA (7).

An alternative to the possibility discussed in the previous paragraph is that the α-helical increase that occurs upon acetylation may play an important role in the modulation of interaction(s) of the core histone tails with chromatin remodeling complexes such as NURF (*Drosophila* nucleosome remodeling factor (55) or the yeast SWI/SNF (switch of the mating type/sucrose nonfermenting, remodeling factor from yeast) and RSC (remodel of the structure of chromatin) complex (56).

Also, it has recently been shown that a small amphipathic α-helical region of approximately 10 amino acids is sufficient for transcriptional activation of Stat5 (57), a transcription factor involved in signal transduction and the activation of transcription. Consequently, relatively small structural changes such as those presented in this paper may have important structural and functional implications.

Over the years, we have been looking for major structural changes in chromatin produced by histone acetylation. It is possible that the structural changes are actually as subtle as the specificity of the enzymes (histone acetyl transferases/histone deacetylases) that bring them about (58, 59).

Acknowledgments—We are grateful to John D. Lewis for skillful computer assistance in the preparation of the figures. We also thank Sandy Kielland of the Protein Microchemistry Center of the University of Victoria (Victoria, British Columbia, Canada) for carrying out the amino acid analyses.

REFERENCES

1. Mizzen, C. A., and Allis, C. D. (1998) *Cell. Life Sci.* **54,** 6–20
2. Garcia-Ramirez, M., Rocchini, C., and Ausió, J. (1995) *J. Biol. Chem.* **270,** 17923- 17928
3. McGhee, J. D., Nickol, J. M., Felsenfeld, G., and Rau, D. C. (1983) *Nucleic Acids Res.* **12,** 4065–4075
4. Dimitrov, S., Makarov, V., Apostolova, T., and Pashev, I. (1986) *FEBS Lett.* **197,** 217–220
5. Ausió, J., and Van Holde, K. E. (1986) *Biochemistry* **22,** 1421–1428
6. Norton, V. G., Imai, B. S., Yau, P., and Bradbury, E. M. (1989) *Cell* **57,** 449–457
7. Mutskov, V., Gerber, D., Angelov, J., Ausió, J., Workman, J., and Dimitrov, S. (1998) *Mol. Cell. Biol.* **18,** 6293–6304
8. Lee, D. Y., Hayes, J. J., Pruss, D., and Wolffe, A. P. (1993) *Cell* **72,** 73–84
9. Howe, L., and Ausió, J. (1998) *Mol. Cell. Biol.* **18,** 1156–1162
10. Panetta, G., Buttinelli, M., Flaus, A., Richmond, T. J., and Rhodes, D. (1998) *J. Mol. Biol.* **282,** 683–697
11. Cirillo, L. A., and Zaret, K. S. (1999) *Mol. Cell.* **4,** 961–969
12. Strahl B. D., and Allis, D. C (2000) *Nature* **403,** 41–45
13. Baneres J. L., Martin, A., and Parelló, J. (1997) *J. Mol. Biol.* **273,** 503–508
14. Prevelige, P. E., Jr., and Fasman, G. D. (1987) *Biochemistry* **20,** 2944–2955
15. Allan, J., Harborne, N., Rau, D. C., and Gould, H. (1982) *J. Cell Biol.* **93,** 285–297
16. Garcia-Ramirez, M., Dong, F., and Ausió, J. (1992) *J. Biol. Chem.* **267,** 19587–1995
17. Hansen, J. C., Tse, C., and Wolffe, A. P. (1998) *Biochemistry* **37,** 17637–17641
18. Spencer, V. A., and Davie, J. R. (1999) *Gene* (*Amst.*) **240,** 1–12
19. Sung, M. T., and Dixon, G. H. (1970). *Proc. Nat. Acad. Sci U. S. A.* **67,** 1616–1623
20. Peng, H. F., and Jackson, V. (1997) *Biochemistry* **36,** 12371–12382
21. Perry, M., and Chalkley, R. (1981) *J. Biol. Chem.* **256,** 3313–3318
22. Ausió, J., Dong, F., and van Holde, K. E. (1989) *J. Mol. Biol.* **206,** 451–463
23. Yager, T. D., and van Holde, K. E. (1984) *J. Biol. Chem.* **259,** 4212–4222
24. Laemmli, U. K. (1970) *Nature* **227,** 680–685
25. Simon, R. H., and Felsenfeld, G. (1979) *Nucleic Acids Res.* **6,** 689–696
26. Li, W., S. Nagaraja, G. P. Decluve, M. J. Hendzel, and Davie, J. R. (1993) *Biochem. J.* **296,** 737–744
27. Ausió, J., and Moore, S. C. (1998) *Methods* **15,** 333–342
28. Carlos, S., Jutglar, L., Borrell, J. I., Hunt, D. F., and Ausió, J. (1993) *J. Biol. Chem.* **268,** 185–194
29. Böhm, L., and Crane-Robinson, C. (1984) *Biosci. Rep.* **4,** 365–386
30. Verdaguer, N., Perelló, M., Palau, J., and Subirana, J. A. (1993) *Eur. J. Biochem.* **214,** 879–887
31. Ausió, J., Seger, D., and Eisenberg, H. (1984) *J. Mol. Biol.* **176,** 77–104
32. Stein, A. (1979) *J. Mol. Biol.* **130,** 103–134
33. Arents, G., Burlingame, R. W., Wang, B.-C., Lowe, W. E., and Moudrianakis, E. N. (1991) *Proc. Natl. Acad. Sci. U. S. A.* **88,** 10148–10152
34. Luger, K., Mäder, A. W., Richmond, R. K., Sargent, D. F., and Richmond, T. J. (1997) *Nature* **389,** 251–260
35. Bradbury, E. M., Cary, P. D., Crane-Robinson, C., Rattle, H. W. E., Boublik, M., and Sautière, P. (1975) *Biochemistry* **14,** 1876–1885
36. Chen, Y.-H., Yang, J. T., and Chau, K. H. (1974) *Biochemistry* **13,** 3350–3359
37. Greenfield, N., and Fasman, G. D. (1969) *Biochemistry* **8,** 4108–4116
38. Eickbush, T. H., and Moudrianakis, E. N. (1978) *Biochemistry* **17,** 4955–4964
39. Walker, I. O. (1984) *Biochemistry* **23,** 5622–5628
40. Zhong, L., and Johnson, W. C., Jr. (1992) *Proc. Nat. Acad. Sci. U. S. A.* **89,** 4462–4465
41. Cary, P. D., Crane-Robinson, C., Bradbury, E. M., and Dixon, G. H. (1982) *Eur. J. Biochem.* **127,** 137–143
42. Yang, J. T., Wu, C. C., and Martinez, H. M. (1986) *Methods Enzymol.* **130,** 208–269
43. Xu, X., Cooper, L. G., DiMario, P. J., and Nelson, J. W. (1995) *Biopolymers* **35,** 93–102
44. Lehrman, S. R., Tuls, J. L., and Lund, M. (1990) *Biochemistry* **29,** 5590–5596
45. Segawa, S., Fukuno, T., Fujiwara, K., and Noda, Y. (1991) *Biopolymers* **31,** 497–509
46. Sonnichsen F. D., Van Eyk, J. E., Hodges, R. S., and Sykes, B. D. (1992) *Biochemistry* **31,** 8790–8798
47. Nelson J. W., and Kallenbach, N. R. (1989) *Biochemistry* **28,** 5256–5261
48. Alder, A. J., and Fasman, G. D. (1974) *J. Biol. Chem.* **249,** 2911–2914
49. Bone, J. R., Lavender, J., Richman, R., Palmer, M. J., Turner, B. M., and Kuroda, M. I. (1994) *Genes Dev.* **8,** 96–104
50. Smith, E. R., Pannuti, A., Gu, W., Steurnagel, A., Cook, R. G., Allis, D. C., and Lucchesi, J. C. (2000) *Mol. Cell. Biol.* **20,** 312–318
51. Johnson, L. M., Fisher-Adams, G., and Grunstein, M. (1992) *EMBO J.* **11,** 2201–2209
52. Candido E. P., and Dixon, G. H. (1971) *J. Biol. Chem.* **246,** 3182–3188
53. Hong, L., Schroth, G. P., Matthews, H. R., Yau, P., and Bradbury, E. M. (1993) *J. Biol. Chem.* **268,** 305–314
54. Puig, O. M., Bellés, E., López-Rodas, G., Sendra, R., and Tordera, V. (1998) *Biochim. Biophys. Acta* **1397,** 79–90
55. Georgel, P. T., Tsukiyama, T., and Wu, C. (1997) *EMBO J.* **16,** 4717–4726
56. Logie, C., Tse, C., Hansen, J. C., and Peterson, C. L. (1999) *Biochemistry* **38,** 2514–2522
57. Wang, D., Moriggl, R., Stravopodis, D., Carpino, N., Marine, J-C., Teglund, S., Feng, J., and Ihle, J. N. (2000) *EMBO J.* **19,** 392–399
58. Johnson, C. A., and Turner, B. M. (1999) *Semin. Cell Dev. Biol.* **10,** 179–188
59. Brown, C. E., Lechner, T., Howe, L., and Workman, J. L. (2000) *Trends Biochem. Sci.* **25,** 15–19
60. Georgieva, E. I., and Sendra, R. (1999) *Anal. Biochem.* **269,** 399–402
61. Fasman, G. D., Chou, P. Y., and Adler, A. J. (1976) *Biophys. J.* **16,** 1201–1238
62. Chou, P. Y., and Fasman, G. D. (1978) *Adv. Enzymol.* **47,** 45–148
63. Deléage, G., and Roux, B. (1987) *Protein Eng.* **1,** 289–294
64. Gilbrat, J. F., Garnier, J., and Robson, B. (1987) *J. Mol. Biol.* **198,** 425–443
65. Eisenberg, D., Weiss, R. M., and Terwilliger, T. C. (1984) *Proc. Natl. Acad. Sci. U. S. A.* **81,** 140–144
66. Creighton, T. E. (1996) *Proteins*, 2nd Ed., W. H. Freeman and Co, New York